The response of nematodes to deep-sea CO_2 sequestration: A quantile regression approach

J. W. Fleeger[1]*, D.S. Johnson[2], K. R. Carman[1], P. B. Weisenhorn[1], A. Gabriele[1], D. Thistle[3], J.P. Barry[4]

[1] Department of Biological Sciences, Louisiana State University, Baton Rouge, Louisiana 70803, USA
[2] Ecosystems Center, Marine Biological Laboratory, 7 MBL St., Woods Hole, MA 02543, USA
[3]Department of Oceanography, Florida State University, Tallahassee, Florida 32306-4320, USA
[4]Monterey Bay Aquarium Research Institute, Moss Landing, California 95039, USA

*Corresponding author. Tel: 225 578-1738; facsimile: 225 578-2597; e-mail address: zoflee@lsu.edu

Running head: Responses of deep-sea nematodes to sequestered carbon dioxide

Abstract

One proposed approach to ameliorate the effects of global warming is sequestration of the greenhouse gas CO_2 in the deep sea. To evaluate the environmental impact of this approach, we exposed the sediment-dwelling fauna at the mouth of the Monterey Submarine Canyon (3262 m) and a site on the nearby continental rise (3607 m) to CO_2-rich water. We measured meiobenthic nematode population and community metrics after ~ 30-day exposures along a distance gradient from the CO_2 source and with sediment depth to infer the patterns of mortality. We also compared the nematode response with that of harpacticoid copepods. Nematode abundance, average sediment depth, tail-group composition, and length: width ratio did not vary with distance from the CO_2 source. However, quantile regression showed that nematode length and diameter increased in close proximity to the CO_2 source in both experiments. Further, the effects of CO_2 exposure and sediment depth (nematodes became more slender at one site, but larger at the other, with increasing depth in the sediment) varied with body size. For example, the response of the longest nematodes differed from those of average length. We propose that nematode body length and diameter increases were induced by lethal exposure to CO_2-rich water and that nematodes experienced a high rate of mortality in both experiments. In contrast, copepods experienced high mortality rates in only one experiment suggesting that CO_2 sequestration effects are taxon specific.

Key words: Carbon dioxide; Nematode body size and shape; Sediment vertical profile; Monterey Canyon; Quantile regression

1. Introduction

Direct ocean carbon sequestration has been proposed as a method to reduce CO_2 emissions to the atmosphere (IPCC, 2005) by impounding carbon in the ocean (Marchetti, 1977; Ormerod *et al*., 2002). Concentrated CO_2 is liquid and denser than seawater at ocean temperatures and pressures found below about 2600 m (Brewer *et al*., 1999), and if injected below this depth, would dissolve into the near-bottom water and remain there for hundreds of years. CO_2-rich seawater would be advected over the seafloor exposing sediment-dwelling organisms to elevated CO_2 concentrations and, because pH decreases as the concentration of CO_2 in seawater increases, increased acidity. Laboratory studies have shown that exposure to CO_2-rich water adversely affects the physiology of shallow-water organisms by causing hypercapnia and/or acidosis (Ishimatsu *et al*., 2004; Kurihara *et al*., 2004). Because natural CO_2 concentrations and pH are much less variable in the deep sea than in shallow water, deep-sea organisms are expected to be more sensitive to perturbations than shallow-water organisms (Shirayama, 1995; Seibel and Walsh, 2001, 2003). Initial reports support this contention (e.g., Tamburri et al., 2000; Pane and Barry, 2007).

Meiobenthic nematodes are good subjects to test for *in situ* CO_2 effects because their small size facilitates sampling in close proximity to release points and because most are poor dispersers, unable to escape exposure. Moreover, nematodes have high abundance, a large diversity of species and functional groups (Thistle et al., 1995; Schratzberger et al., 2007) and a large range in body size (3 orders of magnitude in length and 5 in individual mass) that enhances the potential for detecting effects,

including those that are size related (e.g., Brown et al., 2004). Laboratory fixation studies have shown that nematode body size may be affected by the cause of death (Fagerholm, 1979), suggesting that body size also conveys information regarding morbidity. Fleeger et al. (2006) examined the effects of CO_2-rich water on individual nematode abundance, and body size and shape in release experiment CO_2-4 of Barry et al. (2005). Exposure to CO_2-rich water did not elicit a change in nematode abundance but did cause an increase in the average length and diameter of nematodes. This result suggested that nematodes suffered a high rate of mortality from CO_2 exposure and that in the absence of significant decomposition, changes in body size occurred in association with a lethal exposure.

It is important to determine if the results of experiments that release CO_2 are replicable. In this report, we compare responses of nematodes from the CO_2-4 release experiment, done in Monterey Canyon, with those from a similar experiment done on the nearby continental rise (CO_2-5 of Barry *et al*., 2005). Differences among release experiments may arise due to differences in physical conditions affecting CO_2 dissolution and advection. Thistle et al. (2005) and Sedlacek et al. (2009) concluded that a large proportion of the harpacticoid copepods died in CO_2-4 but not in CO_2-5 and argued that exposure differences occurred. Barry et al. (2005) reported that effects were stronger on benthic flagellates and amoebae in some release experiments than others and also considered variation in CO_2 exposure as a cause. It is also possible, however, that tolerance to CO_2-rich water may not be equivalent in all biota. For example, physiological differences in acid-base regulation may cause taxon-specific sensitivity

(Pane and Barry, 2007). Community composition, body size, body shape, and tail-type groups (Thistle et al., 1995; Tita et al., 1999; Soetaert et al., 2002) of nematodes vary across habitats, and differences in sensitivity to environmental conditions such as food input, sediment composition, oxygen availability, and disturbance (Vanaverbeke et al., 2003; Udalov et al., 2005) may lead to differences in tolerance. The benthic environment and the functional characteristics of nematodes differed at the CO_2-4 and CO_2-5 sites, suggesting a comparison of effects on nematodes (and harpacticoids) would provide a broader view of the impact of carbon sequestration.

Nematode body size and shape vary in response to environmental variation (Vanaverbeke et al., 2004a; 2004b), for example, with depth in the sediment (Jensen, 1987; Soetaert et al., 2002; Soetaert et al., 2009). Previous investigators that examined variation in body size or shape considered the average response, but differences in response across the range of body sizes have not been well characterized. Body-size variation in response to environmental gradients is plausible; the response of a short nematode (e.g., 150 µm in length) to CO_2 exposure may differ from the response of a very long nematode (e.g., 5000 µm in length) because of differences in mobility, anatomy, gas exchange, or physiological processes. To better understand the effects of CO_2 sequestration on deep-sea benthic fauna, we used a powerful statistical technique, quantile regression, to examine how nematodes across their entire size range varied with depth in the sediment and in response to CO_2-rich water.

2. **Methods**

Experiments CO_2-4 and CO_2-5 were both conducted off central California; CO_2-4 was conducted in the axis of lower Monterey Submarine Canyon (36.3781^{o}N, 122.6761^{o}W) at 3262-m depth and CO_2-5 was carried out at 36.709° N 123.523° W at 3607-m depth on the nearby continental rise (Barry et al., 2005 and Figure 1). All manipulations on the seafloor were done with the remotely operated vehicle *Tiburon* of the Monterey Bay Aquarium Research Institute. In CO_2-5, seven 48-cm inner diameter by 15-cm long sections of polyvinyl-chloride pipe (hereafter referred to as corrals) were pushed ~ 3 cm into the seafloor such that their walls were perpendicular to the seabed. Corrals were positioned in a circle 15 m in diameter, and ~20 L of liquid CO_2 were dispensed into each (Barry *et al*., 2005). The same corrals and method of CO_2 release were used in CO_2-4 (Carman *et al*., 2004; Thistle *et al*., 2005; 2006), but the number and arrangement of corrals differed (Figures 2 and 3). In both release experiments, liquid CO_2 from the corrals dissolved over days to weeks into the overlying water, which created a dissolution plume of low-pH, CO_2-rich seawater. As CO_2 hydration occurred, the plume became negatively buoyant (Brewer *et al*., 2005) and flowed over the surrounding sediment surface. We returned ~30 days after the treatment was established. In CO_2-5, we took one 7-cm inner diameter core from the center of a corral (a 0-m sample) and four cores at 2-m (equidistant between two adjacent corrals), 4-m, 8-m, 21-m, and 75-m distances from corrals (Figure 3). In CO_2-4, cores of the same dimensions were collected in corrals, at 2-m and 75-m distances (Figure 2). Replicate samples at each distance were taken from a single deployment of the ROV to the seafloor, and were thus taken within the range of the mechanical arm in close proximity

to each other. Shipboard pH profiles were taken from each core and have been previously reported from corral (Fleeger et al., 2006) and non-corral samples (Thistle et al., 2005; Sedlacek et al., 2009). Sample processing was identical in the two experiments. The upper 30 mm of each core was extruded, and the 0-5, 5-10, 10-20 and 20-30 mm core layers were placed in separate containers before fixation with 10% buffered formalin made from artificial seawater of salinity 35 and buffered with sodium tetraborate. CO_2-4 samples were collected in September and CO_2-5 was sampled in December, reducing the chance that seasonal differences may have influenced outcomes (e.g., nematode body size may respond to seasonal inputs of phytodetritus typically associated with spring phytoplankton blooms, Vanaverbeke et al., 2004a).

In the laboratory, sediment from each core layer was extracted with LUDOX following methods in Carman et al. (2004), and the supernatant and pellet were separately passed through a 32-μm sieve. Retained nematodes from both the supernatant and pellet were enumerated with the use of a stereo-dissection microscope. All nematodes were transferred to glycerin-filled, 15-mm diameter etched wells on microscope slides after rinsing with water to remove residual formalin. Fifty nematodes were placed in each well, except the last well into which any remaining individuals were placed. Cover slips (25 x 25 mm) were placed over the wells. Digital photographs were taken of a subsample of nematodes from each sample-depth combination at appropriate magnification ranging from 5-450 x, on an Olympus BX50 microscope. Fifty nematodes were photographed from each sample-depth combination except from the corral sample (where only 49 nematodes were available in the 0-5 mm

layer), two samples at 2 m (both in the 0-5 mm layer in which 23 and 45 nematodes were available) and one sample at 4 m (in the 0-5 mm layer in which 37 nematodes were available). An approximately equal fraction of the total number of nematodes was photographed from each microscope slide well. To select nematodes to photograph from a well, a slide was examined at 20 x magnification while using the stage manipulator to systematically search for nematodes across the diameter of the slide. Each nematode was photographed with a SPOT RT (model 7.2 Color Mosaic) camera using SPOT RT Software, v 3.5. If the appropriate number of nematodes was not found on the initial pass, a second pass was made. Care was taken not to photograph the same nematode more than once. Examination of photographs revealed that nematodes were cylindrical and retained their natural body shape after transfer to glycerin.

IPLab, v 3.6 software was used as an aid to measure the length and diameter of each nematode. A hand-operated computer mouse was used to measure the length (excluding filiform tails which were defined to begin at the point of the greatest reduction in body diameter at the transition to the more slender tail) and greatest diameter of each nematode. A total of 3950 nematodes were measured in CO_2-5 and 2682 in CO_2-4. Biovolume for each nematode was calculated following Feller and Warwick (1988) in which biovolume (nL) = length (mm) * diameter $(mm)^2$ * 530, and individual dry mass was estimated by using 1.13 g cm^{-3} as the specific gravity and a 0.25 dry to wet weight conversion factor. In addition, each nematode was categorized into one of five tail morphology groups. Following Thistle *et al.* (1995), we established four tail groups; (1) rounded (blunt end), (2) clavate-conicocylindrical (initially conical but

with an extension to the tip), (3) conical (pointed tip with a tail length less than 5 body diameters), and (4) elongate (with a filiform tail longer than 5 body widths). A fifth tail group, tail end ring, was added because nematodes in the family Desmoscolecidae were abundant at the CO_2-5 study site and possessed a tail morphology unlike other nematodes. Nematodes in the Desmoscolecidae are characterized by a tail end ring that creates a "squared off" appearance but with a short tapered or triangular tail that extends posterior to the tail ring.

2.1 *Quantile regression background and statistical methods*

In linear regression models of a biological response (e.g., nematode length) against a measured factor, values should fall more or less on the slope of the line if the measured factor(s) is the only cause of variation. Thus, the measured factor(s) would explain all of the variability found in response variables (i.e., a perfect fit, $R^2 = 1.0$). However, this is rarely, if ever, the case, and the residual (unexplained) variance becomes an error term and is assumed to have a normal distribution. Within this error are effects of unmeasured factors that may influence or interact with measured factors, and regression models that focus on only the middle of the distribution (e.g., least-square estimations) may miss detection of effects at different parts of the response distribution (e.g., 0.90 quantile).

By analyzing various quantiles (points taken at regular intervals from the cumulative distribution function of a random variable such that the f quantile, q_f, of a dataset is a value with an approximate fraction f of the data less than or equal to q_f), quantile regression (Koenker and Basset, 1978) can be used to identify possible

interactions between measured and unmeasured factors (Cade and Noon, 2003). It is possible that the effects of unmeasured factors are simply additive. In such a case, the slopes across all quantiles should be parallel. However, as often is the case, unmeasured factors may interact with measured factors resulting in unequal slopes across quantiles. In heterogeneous distributions, changes in the mean response may not reveal changes that occur at a different portion of the response distribution (Cade et al., 1999). Because quantile regression estimates several slopes, it can identify relationships between variables missed by other models.

Quantile regression has been demonstrated as a useful tool in ecological studies for detecting limiting factors (Cade et al., 1999; Cade and Noon, 2003; Planque and Buffaz, 2008). To understand if a factor is limiting, it is helpful to model the maximum response instead of a mean. Quantile regression allows an investigator to model upper quantiles (tau > 0.90) and thus describe the maximum biological response (e.g., nematode length) to a factor (e.g., sediment depth) rather than just the mean response. In this way, a factor may be considered limiting when slopes of the upper quantiles are steep and significantly different from zero. Quantile regression makes no assumption about the error-term distribution as required in parametric regressions and is robust to outliers. Quantile regression offers the advantage over ordinary least-square models in that it can be used to explore other parts of the response distribution.

In examining marine soft-sediments and/or the deep sea, investigators are unlikely to be able to measure all potential factors influencing fauna. Our focus was on the response of nematodes as a function of their proximity to sequestered CO_2 and their

depth in the sediment. Quantile regression allowed us to examine the possibility of these two factors as limiting factors in the response of nematodes by examining a large range of their response distributions.

Simple linear regressions were modeled for nematode length, diameter, and length: width ratio (L/W) against each factor (distance from the CO_2 source and depth in the sediment), and the significance of the relationships between these variables and factors were tested (H_0: slope=0). Data were analyzed both untransformed and after ln transformation. As an aid, nematode size data were visualized as median values in all figures because of the large variation in nematode body size (about 4 orders of magnitude in individual biovolume). Linear quantile regression was performed for seven selected taus (0.05, 0.10, 0.25, 0.50, 0.75, 0.90, and 0.95) for each morphometric variable against each factor. The slope of each tau was tested against the hypothesis of slope = 0 by invoking a rank-inversion method to generate confidence intervals (Koenker, 2005**)**. ANOVA was used to test the hypothesis that all seven tau's were equal (i.e., had homogenous slopes). Data from the two experiments were analyzed separately. All analyses were done in *R* (R Development Core Team, 2008), and quantiles were fit using 'quantreg,' a library for quantile regression analysis (Koenker, 2008).

Abundance data were standardized to individuals mm^{-1} of core layer (i.e., 0-5, 5-10, 10-20, and 20-30 mm), weighted in the analysis by the number of millimeters represented by the core layer, and expressed as individuals 10 cm^{-2} for all layers. We also estimated the abundance of tail groups 4 and 5 by using tail-morphology-group

frequencies from nematodes subsampled for photography. The proportion of the subsample classified in the tail group was multiplied by the observed total nematode abundance for that layer.

We applied a split-plot ANOVA to nematode counts after ln transformation for all distances from the corral; factors were distance from the CO_2 source and core layer, and interactions were examined. Comparisons among factors were conducted with the Tukey procedure. A weighted-mean depth for nematodes in each sample was calculated to estimate an average depth in mm (Fleeger et al., 1995). One-way ANOVA was used to compare nematode weighted mean depth for all distances from the corral in CO_2-5.

3. **Results**

3.1 *Comparison of nematodes at the CO_2-4 and CO_2-5 study sites*

Nematodes were more abundant at the CO_2-5 site (mean abundances ± 1 s.d. through 3 cm were 450.2 ± 309.8 and 853.8 ± 139.7 ind. 10 cm^{-2} at the CO_2-4 and CO_2-5 sites respectively), but they were larger in individual body size at CO_2-4. Median lengths and diameters pooled across core layers were 776.2 (with a range from 172 to 3951) and 26.2 (range from 6.3 to 147) µm at the CO_2-4 study site and 482.5 (range from 81 to 8167) and 21.3 (range from 3 to 191) µm at the CO_2-5 site. Because nematodes differed in length and diameter, biovolume and individual mass, which were calculated from them, also differed between the study sites. Median biovolumes were 0.279 and 0.170 nL $ind.^{-1}$ at CO_2-4 and CO_2-5 respectively. Overall, nematodes at the two sites ranged from < 0.001 to > 10 µg dry mass $ind.^{-1}$.

At the CO_2-4 site, nematode body shape was dominated by individuals with a long, thin shape (median L/W ratio of about 30). Nematodes at the CO_2-5 site had two distinct shapes; a long, thin shape (median L/W ratio of about 30) and a short, stout shape with a median L/W ratio of about 6 (Figures 4 and 5). At the CO_2-4 study site, nematode tail groups were relatively low in diversity (Fleeger et al., 2006). Two tail groups (conical and elongate) comprised about 72% of all nematodes photographed. Short, stout nematodes in the family Desmoscolecidae (in the tail end ring group) were included in tail group 1 (rounded) in Fleeger et al. (2006). For this paper, we reanalyzed the photographs and found that they were rare at the CO_2-4 site (< 1% of all nematodes). At the CO_2-5 site, tail groups were even more strongly dominated by two groups. Tail groups 1 (rounded), 2 (clavate-conicocylindrical), and 3 (conical) were very rare, together comprising ~8% of nematodes photographed. Tail group 5 (tail end ring) consisted of short, stout (with a median L/W ratio of 6.2) nematodes most of which were in the family Desmoscolecidae and comprised 18.7%; tail group 4 (elongate) nematodes were long and slender (median L/W ratio of 29.7) and comprised 72.9% of all nematodes photographed.

3.2 *Variation with sediment depth*

Tail-group composition differed little with core layer in CO_2-4. Tail group 4 (elongate) was the most frequently encountered group at all depths, ranging from 57-69% of the total. In CO_2-5, the proportion of nematodes with elongate tails increased with increasing core layer, while the proportion of nematodes with a tail end ring decreased with increasing core depth from a peak at 5-10 mm.

Nematodes at the CO_2-5 site were more variable in body dimensions (especially diameter) across the core layers (Figure 6). Simple linear regression suggested that nematode length increased with increasing sediment depth in both CO_2-4 and CO_2-5, and that nematode diameter increased with increasing core layer in CO_2-4 but decreased in CO_2-5 (Table 1; Figure 6 shows relationships as median values). Nematode L/W ratio regressed against sediment depth indicated a significant positive relationship for both experiments (Table 1) but with a steeper slope in CO_2-5 (Figure 6). However, all linear regressions (of raw and ln transformed data) had poor explanatory power ($R^2 \leq$ 0.05; Table 1).

Quantile regression revealed that nematodes in different quantiles for length and L/W ratio, but not diameter, responded differently to sediment depth. The slopes of quantile regressions for nematode length and core layer were significantly positive for taus $\leq$ 0.75, but not significantly different from 0 for tau = 0.90, and significantly negative for tau = 0.95 in CO_2-4 (Table 2, Figure 7). This suggests that nematodes up to 1010 µm (Table 3 provides sizes for various quantiles) progressively increased in length, whereas the longest nematodes (> 1620 µm) decreased in length with increasing sediment depth. Similarly in CO_2-5, the slopes were significantly positive for taus $\leq$ 0.75, but with no relationship between core layer and length in quantiles > 0.90 (Table 2; Figure 7). A majority of the smaller length classes of nematodes (those < 1243 µm) increased in length with increasing sediment depth in CO_2-5. Tests for equality of slopes confirmed that the slopes of the quantile regressions were significantly different in both

experiments (i.e., heterogeneous models, Table 4), and slopes were strongly steeper in the higher quantiles.

For nematode diameter, slopes of quantile regressions were increasingly and significantly positive for all taus for CO_2-4 (Table 2, Figure 7); conversely, all taus were increasingly and significantly negative for CO_2-5 (Table 2, Figure 7). Thus, nematodes in all quantiles (but especially the widest nematodes) were found to be progressively wider with sediment depth at CO_2-4, but nematodes at CO_2-5 were thinner with increasing sediment depth. Tests for equality of slopes confirmed that the slopes of the quantile regressions were significantly different in both experiments (i.e., heterogeneous models, Table 4).

For L/W ratio, slopes of the quantile regressions were significantly positive for taus $\leq$ 0.75 for CO_2-4 with no effect on taus > 0.75. These results indicate that nematodes with values < 35 increased in L/W ratio with increasing sediment depth, but nematodes with values > 35 decreased. Slopes were increasingly and significantly positive for all taus (0.05 – 0.95) for CO_2-5, suggesting that the L/W ratio for nematodes of all sizes increased with increasing depth in the sediment (Table 2; Figure 7). The slopes of the quantiles were significantly different for both experiments indicating heterogeneous models (Table 4).

3.3 *CO_2 effects*

Total nematode abundance and tail group abundance in CO_2-4 were not affected by exposure to CO_2 (Carman et al., 2004; Fleeger et al., 2006). In CO_2-5, highest abundances of nematodes generally occurred at mid-distances from the CO_2 source

(data not shown). Split-plot ANOVA was used to examine distance and core-layer effects on total nematode abundance in CO_2-5. Distance ($p = 0.001$) from the CO_2 source and core layer ($p < 0.001$) both affected nematode abundance without interaction ($p = 0.293$). However, when each distance from the CO_2 source was compared to the most distant sample (75 m), no significant differences were observed ($p > 0.05$ for all comparisons), suggesting variation in abundance was not directly linked to CO_2 exposure. ANOVA also revealed that all core layers differed significantly from each other in abundance. Similar patterns of abundance and trends regarding distance from the CO_2 source and core layer were found for nematodes in the two most abundant tail groups (elongate and tail end ring). Similar to CO_2-4, nematode abundance was highest in the 10-20 mm core layer. The weighted-mean depth of nematodes ranged from 14.7-16.8 mm across the distances sampled from the CO_2 source, and a one-way ANOVA ($p = 0.894$) failed to detect differences in this measure of vertical profile due to CO_2 exposure.

The range in length of nematodes across all individuals measured in CO_2-5 was 81-8167 µm. Median nematode length was 591 µm at 0 m, 625 µm at 2 m, 562 µm at 4 m, 477 µm at 8 m, 464 µm at 21 m and 506 µm at 75 m from the CO_2 source; a difference of 19% between nearest and furthest. Simple linear regression of nematode length against distance from CO_2 source indicated a significant negative relationship for both experiments, i.e., nematodes were longer in samples taken progressively closer to the CO_2 source (Table 1 and Figure 8). However, analysis of raw and ln-transformed data indicated that distance explained little variation ($R^2 \leq 0.01$; Table 1).

Slopes of the quantile regressions between nematode length and distance from the CO_2 source were significantly negative for taus < 0.75 and significantly positive for taus $\geq$ 0.90 for CO_2-4 (Table 5, Figure 8). The steep positive slope for taus $\geq$ 0.90 indicates that nematodes $\geq$ 1324 µm were shorter, but that nematodes ≤ 1010 µm were longer closer to the CO_2 source. The slope of the relationship between nematode length and distance was significantly negative for taus < 0.95 in CO_2-5, indicating that nematodes < 1593 µm increased in length in samples taken progressively closer to the CO_2 source. The slopes of the quantiles increased in the upper quantiles and were significantly different for both experiments, indicating heterogeneous models (Table 4).

The range in nematode diameter was 3-191 µm in CO_2-5. When pooled across all tail groups and layers, the median diameter of nematodes was 25.4 µm at 0 m, 24.2 µm at 2 m, 23.7 µm at 4 m, 21.3 µm at 8 m, 23.0 µm at 21 m and 19.8 µm at 75 m. This represents a 22% increase in the diameter of nematodes when comparing samples nearest to and furthest from the CO_2 source. Simple linear regression of nematode diameter against distance from CO_2 source indicated a significant negative relationship for both experiments (Table 1 and Figure 8). Analysis of raw and ln-transformed data indicated distance explained little of the variation ($R^2 \leq 0.02$, Table 1).

The slopes of the quantile regressions of nematode diameter with distance were significantly negative for taus $\leq$ 0.90 for both experiments (Table 5; Figure 9). This result suggests that for all but the widest (> 57 µm for CO_2-4 and > 62 µm for CO_2-5), nematodes increased in diameter as samples were taken progressively closer to the CO_2

source. The hypothesis of equal slopes of the quantile regressions was rejected for both experiments, suggesting heterogeneous models (Table 4).

The range in L/W ratio among nematodes was 3.14-131.6 in CO_2-5. Median L/W ratios were generally similar at all distances from the CO_2 source and were 27.0 at 0 m, 29.1 at 2 m, 26.7 at 4 m, 25.5 at 8 m, 24.9 at 21 m and 28.4 at 75 m. L/W frequency distributions at each distance were similar in shape and central tendencies (Figure 5). The simple linear regression of nematode L/W ratio against distance from CO_2 source indicated a significant positive relationship for CO_2-4, but the relationship was not significant in CO_2-5 (Table 1 and Figure 8). Analysis of raw and ln-transformed data indicated distance explained little of the variation ($R^2 \leq 0.01$, Table 1).

The only quantile regression slope for L/W ratio versus distance that was significantly different from 0 was tau = 0.95 (positive) for CO_2-4; none was significant in CO_2-5 (Table 5, Figure 9). Although the slopes of the quantile regressions were not equal (Table 4), the above results suggest that CO_2 exposure had little effect on the L/W ratio of these nematodes in both experiments.

The pattern of variation in length, diameter, and L/W ratio across the core layers was similar at all distances from the CO_2 source (Figure 10), although nematodes were slightly longer and wider in samples closest to the CO_2 source in all core layers. This pattern suggests that effects of CO_2 exposure on nematode body size were similar across the vertical gradient and that the two factors acted in an additive fashion.

4. **Discussion**

4.1 *Nematode comparisons in CO_2-4 and CO_2-5*

The body sizes and shapes of nematodes in Monterey Canyon (CO_2-4) at 3262 m depth were very different from those at 3607 m depth on the continental rise (CO_2-5), even though the sites were only ~ 80 km apart. Canyon nematodes differed from published descriptions from the deep sea (Soetaert et al., 2002); they were longer than average, composed primarily of a long, slender body shape (the abundance of short, stout nematodes was low) and diameter increased with depth in the sediment. Nematodes on the continental rise were smaller in size and biovolume, and short, stout nematodes (mostly in the family Desmoscolecidae) were much more common. Length medians for CO_2-5 were similar to those reported by Soetaert et al. (2002) for the deep sea, and bimodal peaks in L/W ratio (Figures 4 and 5) were at similar values. Thus, nematodes from our continental rise station coincided with the body size patterns proposed for the deep sea, whereas nematodes from the canyon more closely resembled patterns described for the continental shelf and slope (Soetaert et al., 2002). Body size in nematodes is related to trophic conditions and sediment properties as well as water depth (Udalov et al., 2005; Soetaert et al., 2009). Taken together, these observations suggest that functional differences among nematodes occurred between the two sites (Schratzberger et al., 2007).

4.2 *Body size variation with sediment depth*

We examined changes in nematode body size and shape across the vertical sediment profile at two locations partially affected by CO_2-rich water. Nematode body size increased at distances close to the source of CO_2. However, the magnitude of the increase was very similar in both experiments, and CO_2 exposure did not affect

nematode L/W ratio (see section 4.3). Furthermore, CO_2-induced changes in nematode morphometrics were similar in all core layers in both experiments (Fleeger et al., 2006, and Figure 10), suggesting additive effects of CO_2 exposure and sediment depth on body size. Although our absolute measurements of median length and diameter from this study are biased because of CO_2 exposure and are therefore not comparable with other deep-sea locations, changes in body size with sediment depth were similarly influenced by CO_2 exposure at both locations. Therefore, trends in nematode morphometrics with sediment depth are comparable between the two release experiments.

Variation in nematode body size and shape across the sediment vertical profile has been described by two contrasting patterns in marine benthic environments. In permeable sands (Jensen, 1987) and in oxygen-rich sediments of the deep sea (Soetaert et al., 2002), nematodes on average are found to be longer and/or thinner with increasing sediment depth, but in oxygen-poor continental shelf/slope muds, nematodes on average are found to be progressively larger with increasing sediment depth (Soetaert et al., 2002). The cause of these differences in vertical profile has been attributed to chemical gradients associated with oxygen (Teiwes et al., 2007) and/or redox distribution, coupled with size-related differences in nematode mobility (Soetaert et al., 2002). Our results also suggest a relationship with chemical gradients as nematodes on average at CO_2-5 (a site similar to other deep-sea sites that experience deep oxygen penetration, Reimers et al., 1986) were thinner with increasing sediment depth while at CO_2-4 (with oxygen penetration limited to the upper centimeter, Barry unpublished) nematodes on average were longer and wider with increasing sediment

depth. No studies have simultaneously examined nematode morphometrics and chemical profiles from contrasting habitats, but such studies would improve our understanding of these patterns.

Quantile regression revealed that relationships with sediment depth varied across the range of body size at both locations. Very long nematodes either did not respond to vertical profile or responded in the opposite fashion than shorter nematodes; e.g., very long nematodes (≥ 1620 μm and ≥ 0.95 quantile) were found to be shorter with increasing sediment depth at CO_2-4, while the average nematode was found to be longer. Similarly, the response to vertical profile differed with body shape at CO_2-4, where nematodes with a large L/W ratio (> 35 μm and ≥ 0.75 quantile) responded in the opposite fashion than the average nematode. In contrast, nematodes across all diameter quantiles varied similarly with sediment depth at both study sites even though diameter increased at one location but decreased at the other with sediment depth. No other studies have examined how different sizes of nematodes respond to sediment depth, but very large nematodes certainly responded to environmental factors differently than small nematodes at both sample sites. Such a conclusion is perhaps not surprising given the large range in nematode body size (i.e., ~5 orders of magnitude in individual mass) and the general importance of body size in ecology (Brown et al., 2004).

In addition, our results suggest that body shape in nematodes is a complex function because length and diameter responded to sediment depth differently from each other in the two environments. Length and diameter variation probably have

different ecological costs and benefits for nematodes. For example, longer nematodes are likely more mobile than shorter nematodes, perhaps with the ability to make forays below the shallow oxic zone in muddy sediment (Moodley et al., 2000). Shorter nematodes may be limited to a more narrow depth range above the redox zone (Soetaert et al., 2002). Diffusion rates across the body wall are higher in smaller-diameter nematodes (Powell, 1989), and nematode diameter may be influenced by the size of sediment pore spaces (Tita et al., 1999). Length and diameter may therefore respond to different selective forces, and body shape in a given habitat may be the result of a combination of factors influencing each. Overall, our results suggest that the relationship between nematode body size and shape with sediment depth is more complex than previously thought and may be partly related to the large range in body sizes of nematodes.

4.3 *CO_2 effects*

Nematode responses were strikingly similar in both CO_2-release experiments, even though ambient nematode body shape and size, morphometric variation with sediment depth profile, and tail-group types differed. Nematode length and diameter were correlated with distance from the CO_2 source, but distance did not affect nematode abundance (total abundance or absolute or relative abundance of tail types), body shape, or vertical profile within the upper 30 mm in either experiment. In both experiments, average nematode length and diameter increased in samples taken progressively closer to the CO_2 source. The effects of exposure to CO_2 also differed with body size in both release experiments in similar ways. The longest and widest

nematodes (≥ 0.90 quantile) either did not differ or differed in a manner opposite to that of nematodes in the ≤ 0.75 quantile.

Inside corrals, nematodes experienced extreme environmental conditions especially for the deep sea. A pH of 5.4 was recorded in a corral core in CO_2-5 (Fleeger et al., 2006) and pH probably spiked to lower values (Barry et al., 2005) during the ~30-day exposure period in both release experiments. Takeuchi et al. (1997) found that a pH of 5.4 caused approximately 50% mortality after one day of exposure and about 90% mortality after four days of exposure for three species of shallow, subtidal nematodes. In the corral we studied, nematodes did not escape by emerging into the water column (Carman unpublished data from emergence traps) or by burrowing deeper into sediment (as evidenced by a lack of change in vertical profile). The corral walls also kept nematodes from escaping laterally through the sediment. For these reasons, we infer that nematodes in corrals in both experiments suffered very high mortality rates. Quantile regression suggested that distance from the CO_2 source acted as a limiting factor for length and diameter in both experiments, and patterns of variation in nematode body size in corrals were identical to those at sites close to the corrals (2 and/or 4 m from the source). The fact that nematode lengths and diameters in corrals, where we know the nematode mortality must have been severe, were similar to the lengths and widths in sediment close to the source of CO_2 but differed from those further away, suggests that nematodes near the source of CO_2 were also killed in large numbers by it.

In the above, we have followed Fleeger et al. (2006) and interpreted the increase in average nematode length and diameter in sediments exposed to CO_2-rich water as arising because of postmortem changes in nematode morphology. The pattern could also arise if nematodes from sediment depths below that at which CO_2-induced mortality occurred migrated upward after those in the surface sediments died. Such a migration could maintain the pre-CO_2 exposure abundance and vertical profile after a mortality event in the upper 30 mm where we sampled. Nematodes living below 30 mm usually differ in body size from surface-dwelling nematodes on the continental shelf and deep sea (Figure 4a, Soetaert et al., 2002). If longer and wider nematodes from deeper sediments, as we observed in CO_2-4, replaced surface dwellers after CO_2 exposure, nematode length and diameter would increase. However this does not explain our results for CO_2-5 where nematodes increased in length but *decreased* in diameter with increasing sediment depth, at least through 30 mm.

Alternatively, nematodes in sediment near the source of CO_2 during both CO_2-4 and CO_2-5 were killed by CO_2 exposure, but neither decomposition nor recruitment changed the nematode fauna detectably during the ~30 d-duration of the experiments (see Fleeger et al., 2006). The lack of change in community metrics including L/W ratio, tail type, mean depth, and abundance support the idea that the nematodes present before the CO_2 release died in place. In that case, the increase in average length and width resulted from postmortem changes in nematode body size (Fagerholm, 1979). Our data do not allow us to discriminate between the two competing explanations, but both suggest that variation in nematode body size is related to mortality. Thus,

nematodes from the two release experiments exhibited functional characteristics associated with the deep sea (CO_2-5) and the slope/shelf (CO_2-4) respectively, suggesting that nematodes from a broad portion of the sediment-covered deep sea would be adversely affected by carbon sequestration.

We do not know why large nematodes (≥ 0. 90 quantile for length, diameter and L/W ratio) responded differently than small nematodes (≤ 0.75 quantile) to the CO_2 exposure gradient. One explanation may be that large nematodes suffered lower mortality rates. Diffusion varies with body size of small organisms such as nematodes (Powell, 1989; Brown et al., 2004), and CO_2 or H^+ uptake by large nematodes may have been reduced by a slower diffusion rate or by a cuticle with lower permeability. Acid-base regulation in large nematodes may also moderate mortality. Studies with *Caenorhabiditis elegans*, a terrestrial nematode, indicate that external pH influences the transcriptional profile of carbonic anhydrases, possibly enhancing protection from pH change (Hall et al., 2008). Marine nematodes (Riemann and Schrage, 1988) and *C. elegans* have been shown to sense and respond to CO_2 separately from pH, and *C. elegans* exhibits a complex avoidance behavior to CO_2 related to oxygen and food intake (Bretscher et al., 2008). Large nematodes are probably more mobile than small nematodes (Soetaert et al., 2002) and may be better able to use an ability to sense CO_2 and avoid harmful conditions, for example, by using vertical movements in the sediment. Although our data do not suggest a mechanism, our analysis suggests that not all nematodes will respond equally to sequestered CO_2 and that the difference in response is related to body size.

In the CO_2-4 release experiment, mortality to copepods and nematodes close to the source was high, and we suggest here that nematodes experienced high mortality from exposure to CO_2 in the CO_2-5 experiment. In contrast, Sedlacek et al. (2009) found no evidence that exposure to CO_2 caused harpacticoid copepods to die during experiment CO_2-5. These observations suggest that at least some nematodes were less tolerant than harpacticoids. Based on pH pore-water profiles, the exposure to CO_2-rich water by infauna differed in the two experiments. In CO_2-4, pore-water profiles in near samples revealed a reduction in pH by about 0.75 in surface sediment ~30 days after the release, but similar measurements in CO_2-5 gave no indication of a pH gradient from the source of the CO_2 (Sedlacek et al., 2009). However, lower pH values likely occurred earlier in the 30-d duration of both experiments. Barry et al. (2005) found that the pH of near-bottom water close to CO_2 release sites varied over short intervals and that the greatest variation from the norm occurred within the first few days after release as CO_2 dissolution began. Thus, nematodes 2 and 4 m from the CO_2 source may have been exposed to more variable and stressful conditions for pH, suggesting some deep-sea nematodes are intolerant of even short-term exposure to increased acidity. Calcareous foraminiferans were greatly reduced in abundance up to 10 cm in sediment depth in corrals in CO_2-5 (Ricketts et al., 2009). Bernhard et al. (2009) concluded that survivorship rates of agglutinated and thecate foraminifera were not significantly impacted in corrals but the survivorship of calcareous foraminifera was significantly lower in corrals in CO_2-5. It seems very likely that taxon-specific responses to CO_2 sequestration will occur in the deep sea.

Quantile regression provided useful insight to describe the effects of a CO_2-exposure gradient on nematode morphometrics and the response of body size and shape to the sediment-depth gradient. We showed that the response of nematodes along both gradients varied with body size as the largest (longest and largest L/W ratio) nematodes behaved differently compared to the average, and that nematode body size and shape were sensitive measures of environmental effects. Although the reasons for size-related differences in response are unclear, investigations that measure size structure have the potential to greatly improve our understanding of environmental influences on nematodes. Finally, quantile regression strongly implicated CO_2 exposure as a limiting factor to nematodes in both release experiments, suggesting that CO_2 sequestration in deep-sea, near-bottom water to mitigate the Greenhouse effect would negatively impact this most abundant group of sediment-dwelling metazoans.

Acknowledgements

The captain and crew of the R/V *Western Flyer,* the ROV *Tiburon* team, K. Buck, L. Kuhnz, C. Lovera, and P. Whaling aided in the field or laboratory. The paper was improved by comments by P.-Y. Pascal. We thank T. Marshall, A. White, and J. Hathorn for help in sample processing and D. Blouin for statistical consultation. The Department of Energy Office of Biological and Environmental Research supported this research under award numbers DE-FG02-05ER64070 and DE-FG03-01ER63065 and the U.S. Department of Energy, Fossil Energy Group (award DE-FC26-00NT40929). We also appreciate significant support provided by the Monterey Bay Aquarium Research Institute (project 200002).

References

Barry, J. P., K. R. Buck, C. F. Lovera, L. Kuhnz, and P. Whaling., 2005. Utility of deep-sea CO_2 release experiments in understanding the biology of a high CO_2 ocean: Effects of hypercapnia on deep-sea meiofauna. Journal of Geophysical Research Oceans 110, C09S03.

Bernhard, J.M., J.P. Barry, K.R. Buck, and V.R. Starczak., 2009. Impact of intentionally injected carbon dioxide hydrate on deep-sea benthic foraminiferal survival. Global Change Biology 15,2078-2088.

Bretscher, A. J., K. E. Busch, and M. de Bono., 2008. A carbon dioxide avoidance behavior is integrated with responses to ambient oxygen and food in *Caenorhabditis elegans*. Proceedings of the National Academy of Sciences of the United States of America 105, 8044-8049.

Brewer, P. G., C. Friederich, E. T. Peltzer, and F. M. Orr., 1999. Direct experiments on the ocean disposal of fossil fuel CO2. Science 284, 943-945.

Brewer, P. G., E. T. Peltzer, P. Walz, I. Aya, K. Yamane, R. Kojima, Y. Nakajima, N. Nakayama, P. Haugan, and T. Johannessen., 2005. Deep ocean experiments with fossil fuel carbon dioxide: Creation and sensing of a controlled plume at 4 km depth. Journal of Marine Research 63, 9-33.

Brown, J. H., J. F. Gillooly, A. P. Allen, V. M. Savage, and G. B. West., 2004. Toward a metabolic theory of ecology. Ecology 85, 1771-1789.

Cade, B.S., J.W. Terrell, R.L. Schroeder., 1999. Estimating effects of limiting factors with regression quantiles. Ecology 80, 311-323.

Cade, B.S. and Noon, B.R., 2003. A gentle introduction to quantile regression for ecologists. Frontiers in Ecology and the Environment 1, 412-420.

Carman, K. R., D. Thistle, J. W. Fleeger, and J. P. Barry., 2004. Influence of introduced CO_2 on deep-sea metazoan meiofauna. Journal of Oceanography 60, 767-772.

Fagerholm, H.-P., 1979. Nematode length and preservatives, with a method for determining the length of live specimens. Journal of Parasitology 65, 334-335.

Feller, R. J., and R. M. Warwick., 1988. Energetics. Pages 181-196 *in* R. P. Higgins, and H. Thiel editors. Introduction to the Study of Meiofauna. Smithsonian Institution Press, Washington D.C.

Fleeger, J. W., K. R. Carman, P. B. Weisenhorn, H. Sofranko, T. Marshall, D. Thistle, and J. P. Barry., 2006. Simulated sequestration of anthropogenic carbon dioxide at a

deep-sea site: effects on nematode abundance and biovolume. Deep-Sea Research Part I. Oceanographty Research. 53, 1135-1147.

Fleeger, J. W., T. C. Shirley, and J. N. McCall., 1995. Fine-scale vertical profiles of meiofauna in muddy sediments. Canadian Journal of Zoology 73, 1453-1460.

Hall, R. A., D. Vullo, A. Innocenti, A. Scozzafava, C. T. Supuran, P. Klappa, and F. A. Muhlschlegel., 2008. External pH influences the transcriptional profile of the carbonic anhydrase, CAH-4b in *Caenorhabditis elegans*. Molecular and Biochemical Parasitology 161, 140-149.

IPCC (Intergovernmental Panel on Climate Change)., 2005. Carbon dioxide capture and storage, a technical report. /http://www. ipcc.ch/pdf/special-reports/srccs/srccs_technicalsummary.pdf

Ishimatsu, A., T. Kikkawa, M. Hayashi, K. S. Lee, and J. Kita., 2004. Effects of CO2 on marine fish: Larvae and adults. Journal of Oceanography 60, 731-741.

Jensen, P., 1987. Differences in microhabitat, abundance, biomass and body size between oxybiotic and thiobiotic free-living marine nematodes. Oecologia 71, 564-567.

Koenker, R., 2008. quantreg: Quantile Regression. R package version 4.24. http://www.r-project.org

Koenker, R. and Basset, G., Jr., 1978. Regression quantiles. Econometrica 46:33-50

Kurihara, H., S. Shimode, and Y. Shirayama., 2004. Sub-Lethal Effects of Elevated Concentration of CO_2 on Planktonic Copepods and Sea Urchins. Journal of Oceanography 60, 743-750.

Marchetti, C., 1977. On geoengineering and the CO_2 problem. Climate Change 1, 59-69.

Moodley, L., G. T. Chen, C. Heip, and M. Vincx., 2000. Vertical distribution of meiofauna in sediments from contrasting sites in the Adriatic Sea: Clues to the role of abiotic versus biotic control. Ophelia 53, 203-212.

Ormerod W.G., Ferund P. & Smith A., 2002. Ocean storage of CO_2. 2nd Edition. Cheltenham, IEA Greenhouse Gas R&D Programme

Pane, E. F., and J. P. Barry., 2007. Extracellular acid-base regulation during short-term hypercapnia is effective in a shallow-water crab, but ineffective in a deep-sea crab. Marine Ecology Progress Series 334, 1-9.

Planque, B. and Buffaz, L., 2008. Quantile regression models for fish recruitment-environment relationships: four case studies. Marine Ecology Progress Series 357, 213-223.

Powell, E. N., 1989. Oxygen, sulfide and diffusion: Why thiobiotic meiofauna must be sulfide-insensitive first-order respirers. Journal of Marine Research 47, 887-949.

R Development Core Team., 2008. R: A language and environment for statistical computing. R Foundation for Statistical Computing, Vienna, Austria. ISBN 3-900051-07-0, URL http://www.R-project.org.

Ricketts, E.R., J.P. Kennett, T.M. Hill, and J.P. Barry., 2009. Effects of carbon dioxide sequestration on California margin deep-sea foraminiferal assemblages. Marine Micropaleontology 72,165-175

Riemann F., M. Schrage., 1988. Carbon dioxide as an attractant for the free-living marine nematode *Adoncholaimus thalassophygas*. Marine Biology 98,81-86

Reimers C.E., Fischer K.M., Merewether R., Smith K.L., Jahnke R.A., 1986. Oxygen microprofiles measured In situ in deep ocean sediments. Nature 320, 741-744

Schratzberger, M., K. Warr, and S. I. Rogers., 2007. Functional diversity of nematode communities in the southwestern North Sea. Marine Environmental Research 63, 368-389.

Sedlacek, L., D. Thistle, K. R. Carman, J. W. Fleeger, and J. P. Barry., 2009. Effects of carbon dioxide on deep-sea harpacticoids revisited. Deep Sea Research Part I. Oceanography Research. 56, 1018-1025.

Seibel, B. A., and P. J. Walsh., 2001. Potential impacts of CO_2 injection on deep-sea biota. Science 294, 319-320.

Seibel, B. A., and P. J. Walsh., 2003. Biological impacts of deep-sea carbon dioxide injection inferred from indices of physiological performance. Journal of Experimental Biology 206, 641-650.

Shirayama, Y., 1989. Ecology of deep-sea meiobenthos in the western Pacific. Journal of the Oceanographical Society of Japan 45, 83-93.

Shirayama, Y., 1995. Current status of deep-sea biology in relation to CO_2 disposal. Pages 253-264 *in* N. Handa, and T. Ohsumi editors. Direct Ocean Dispersal of Carbon Dioxide. TERRAPUB, Tokyo.

Soetaert, K., A. Muthumbi, and C. Heip., 2002. Size and shape of ocean margin nematodes: morphological diversity and depth-related patterns. Marine Ecology-Progress Series 242, 179-193.

Soetaert, K., M. Franco, N. Lampadariou, A. Muthumbi, M. Steyaert, L. Vandepitte, E. Vanden Berghe, and J. Vanaverbeke., 2009. Factors affecting nematode biomass, length and width from the shelf to the deep sea. Marine Ecology-Progress Series 392,123-132.

Takeuchi K., Y. Fujioka, Y. Kawasak, Y. Shirayama., 1997. Impacts of high concentration of CO_2 on marine organisms; A modification of CO_2 ocean sequestration. Energy Conversion and Management 38,S337-S341

Tamburri, M. N., E. T. Peltzer, G. E. Friedrich, I. Aya, K. Yamane, and P. G. Brewer., 2000. A field study of the effects of CO_2 ocean disposal on mobile deep-sea animals. Marine Chemistry 72, 95-101.

Teiwes, M., M. Bergtold, and W. Traunspurger., 2007. Factors influencing the vertical distribution of nematodes in sediments. Journal of Freshwater Ecology 22,429-439.

Thistle, D., K. R. Carman, L. Sedlacek, P. G. Brewer, J. W. Fleeger, and J. P. Barry., 2005. Deep-ocean, sediment-dwelling animals are sensitive to sequestered carbon dioxide. Marine Ecology Progress Series 289, 1-4.

Thistle, D., P. J. D. Lambshead, and K. M. Sherman., 1995. Nematode tail-shape groups respond to environmental differences in the deep sea. Vie et Milieu - Life and Environment 45, 107-115.

Thistle, D., L. Sedlacek, K. R. Carman, J. W. Fleeger, P. G. Brewer, and J. P. Barry., 2006. Simulated sequestration of industrial carbon dioxide at a deep-sea site: effects on harpacticoid-copepod species. Journal of Experimental Marine Biology and Ecology 330, 151-158.

Tita, G., M. Vincx, and G. Desrosiers., 1999. Size spectra, body width and morphotypes of intertidal nematodes: an ecological interpretation. Journal of the Marine Biological Association of the United Kingdom 79, 1-9.

Udalov, A. A., A. I. Azovsky, and V. O. Mokievsky., 2005. Depth-related pattern in nematode size: What does the depth itself really mean? Progress in Oceanography 67, 1-23.

Vanaverbeke, J., K. Soetaert, and M. Vincx., 2004a. Changes in morphometric characteristics of nematode communities during a spring phytoplankton bloom deposition. Marine Ecology Progress Series 273, 139-146.

Vanaverbeke, J., M. Steyaert, K. Soetaert, V. Rousseau, D. Van Gansbeke, J.-Y. Parent, and M. Vincx., 2004b. Changes in structural and functional diversity of nematode communities during a spring phytoplankton bloom in the southern North Sea. Journal of Sea Research 52, 281-292.

Vanaverbeke, J., M. Steyaert, A. Vanreusel, and M. Vincx., 2003. Nematode biomass spectra as descriptors of functional changes due to human and natural impact. Marine Ecology Progress Series 249, 157-170.

Table 1: Least square regression estimates of slope and intercept, 95% confidence interval (CI), and p-value for H_0: slope=0. Here *y* is one of four variables of nematode morphometrics and *x* is either distance from the CO_2 source or core layer in two CO_2-release experiments. Significance is denoted by asterisks in footnote.

		CO_2-4				CO_2-5			
Response Variable (x)	Factor	Model y=	Lower 95% CI	Upper 95% CI	R^2	Model y=	Lower 95% CI	Upper 95% CI	R^2
Length	Distance	-0.53x+854.61	-1.42	0.35	0.00	-1.04x+681.54	-1.59	-0.05	0.00***
	Layer	45.98x+727.14	30.65	61.32	0.01**	30.41x+582.91	17.17	43.65	0.00***
Ln Length	Distance	0.00x+6.65	0.00	0.00	0.01**	0.00x+6.32	0.00	0.00	0.01***
	Layer	0.07x+6.42	0.06	0.09	0.02**	0.06x+6.13	0.04	0.08	0.01***
Diameter	Distance	-0.08x+31.45	-0.12	-0.04	0.01**	-0.05x+28.47	-0.07	-0.03	0.01***
	Layer	1.55x+26.03	0.79	2.30	0.01**	-3.49x+36.18	-3.94	-3.03	0.05***
Ln Diameter	Distance	0.00x+3.49	0.00	0.00	0.02**	0.00x+3.21	0.00	0.00	0.01***
	Layer	0.04x+3.19	0.03	0.06	0.01**	-0.13x+3.49	-0.15	-0.12	0.07***
L/W Ratio	Distance	0.03x+29.43	0.01	0.06	0.00*	0.02x+29.22	-0.01	0.04	0.00
	Layer	0.78x+28.01	0.33	0.12	0.00**	5.78x+15.02	5.25	6.31	0.10***
Ln L/W Ratio	Distance	0.00x+3.31	0.00	0.00	0.00	0.00x+3.12	0.00	0.00	0.00
	Layer	0.03x+3.23	0.02	0.05	0.01**	0.19x+2.65	0.17	0.21	0.08***

*$p \leq 0.05$, **$p \leq 0.01$, ***$p \leq 0.001$

Table 2. Estimates of the slope, intercept, and 95% confidence intervals (CI) for the H_0: slope=0 from rank-score tests for seven selected regression quantiles. Here *y* is one of four variables of nematode morphometrics and *x* is core layer across the sediment vertical gradient in two CO_2-release experiments. Significance is denoted by asterisks in footnote.

	CO_2-4				CO_2-5			
Response Variable (y)	Quantile	Model y=	Lower 95% CI	Upper 95% CI	Quantile	Model y=	Lower 95% CI	Upper 95% CI
Length	5th***	46.77x+245.33	34.61	61.03	5th***	9.24x+177.39	-4.47	16.98
	10th***	45.63x+307.46	37.66	55.04	10th***	16.37x+197.89	10.60	23.77
	25th***	61.37x+391.36	51.61	77.28	25th***	27.54x+278.97	19.14	38.15
	50th***	79.83x+572.91	69.90	90.86	50th***	42.73x+422.15	30.91	50.26
	75th***	55.19x+854.29	40.25	70.87	75th***	60.21x+662.73	45.00	70.87
	90^{th}	-5.10x+1337.77	-29.82	15.27	90th	12.89x+1206.66	-16.29	55.70
	95th*	-97.32x+1885.42	-123.27	-42.37	95th	-28.31x+1663.37	-46.67	2.42
Diameter	5th***	0.86x+12.47	0.60	1.14	5th***	-1.41x+14.08	-1.86	-0.95
	10th***	0.97x+13.99	0.71	1.21	10th***	-1.38x+15.95	-1.79	-1.12
	25th***	0.95x+17.99	0.64	1.27	25th***	-1.93x+21.40	-2.33	-1.68
	50th**	0.65x+24.53	0.26	1.09	50th***	-3.23x+30.76	-3.68	-2.91
	75th**	0.96x+31.31	0.37	1.63	75th***	-4.38x+44.34	-4.91	-3.95
	90th***	2.97x+40.02	0.85	4.13	90th***	-6.90x+64.93	-7.62	-5.93
	95th***	3.30x+49.62	2.03	5.00	95th***	-4.42x+71.14	-5.26	-2.45
L/W Ratio	5th***	1.61x+12.89	1.30	1.88	5th***	0.59x+3.94	0.47	0.74
	10th***	1.41x+15.04	1.13	1.65	10th***	0.96x+4.09	0.72	1.17
	25th***	1.27x+19.00	0.98	1.54	25th***	4.76x+4.96	4.02	5.36
	50th***	1.17x+24.34	0.83	1.51	50th***	3.65x+17.45	3.24	4.01
	75th***	1.31x+31.16	0.95	1.88	75th***	4.95x+25.31	4.48	5.62
	90th	-0.53x+45.81	-1.39	0.15	90th***	13.31x+23.56	12.45	14.42
	95th	-1.73x+55.68	-3.24	-0.16	95th***	16.00x+26.96	15.17	16.76

*$p \leq 0.05$, **$p \leq 0.01$, ***$p \leq 0.001$

Table 3. Values for selected quantiles for nematode morphometrics from two CO_2 release experiments.

Response Variable	Quantile	CO_2-4	CO_2-5
Length (µm)	5th	357	200
	10th	413	234
	25th	534	349
	50th	776	530
	75th	1010	813
	90th	1324	1243
	95th	1620	1593
Diameter (µm)	5th	14	10
	10th	16	12
	25th	21	16
	50th	26	23
	75th	34	34
	90th	47	50
	95th	57	62
L/W Ratio	5th	17	5
	10th	19	6
	25th	22	17
	50th	27	27
	75th	35	37
	90th	44	54
	95th	51	75

Table 4. Quantile regression of deviance, joint test of equality of slopes for taus = 0.05, 0.10, 0.25, 0.50, 0.75, 0.90, 0.95 from two CO_2-release experiments. These ANOVAs test for equality of slopes of selected taus. Significance is denoted by asterisks in footnote.

Response Variable	Factor	CO_2-4			CO_2-5		
		DF	Residual DF	F-value	DF	Residual DF	F-value
Length	Distance	6	18,761	6.63***	6	29,023	2.43*
	Depth	6	18,761	8.09***	6	29,023	10.23***
Diameter	Distance	6	18,761	2.40*	6	29,023	2.18*
	Depth	6	18,761	2.23*	6	29,023	18.99***
L/W Ratio	Distance	6	18,761	2.60*	6	29,023	2.41*
	Depth	6	18,761	3.86***	6	29,023	94.21***

*$p \leq 0.05$, **$p \leq 0.01$, ***$p \leq 0.001$

Table 5. Estimates of the slope and intercept, 95% confidence intervals (CI), and p-values for the H_0: slope=0 from rank-score tests for seven selected regression quantiles. Here *y* is one of four variables of nematode morphometrics and *x* is distance from the CO_2 source in two CO_2-release experiments. Significance is denoted by asterisks in footnote.

	CO_2-4				CO_2-5			
Response Variable (y)	Quantile	Model y=	Lower 95% CI	Upper 95% CI	Quantile	Model y=	Lower 95% CI	Upper 95% CI
Length	5th***	-2.35x+405.60	-2.66	-1.62	5th***	-0.36x+207.08	-0.60	-0.18
	10th***	-2.02x+456.26	-2.52	-1.60	10th***	-0.38x+243.08	-0.58	-0.20
	25th***	-2.38x+577.44	-3.04	-1.71	25th***	-0.68x+365.49	-1.06	-0.41
	50th***	-2.82x+819.33	-3.47	-2.18	50th***	-0.79x+545.41	-1.12	-0.45
	75th	-0.84x+1021.14	-1.63	0.25	75th***	-1.49x+845.89	-1.49	-2.09
	90th**	3.01x+1276.83	1.46	4.42	90th**	-2.5x+1282.28	-3.58	-1.05
	95th*	6.59x+1506.97	1.97	13.45	95th	-0.97x+1610.38	-2.83	0.73
Diameter	5th***	-0.05x+15.50	-0.07	-0.04	5th***	-0.06x+11.73	-0.06	-0.05
	10th***	-0.07x+17.91	-0.08	-0.05	10th***	-0.05x+13.14	-0.06	-0.04
	25th***	-0.08x+22.33	-0.11	-0.07	25th***	-0.04x+16.62	-0.05	-0.03
	50th***	-0.09x+27.44	-0.11	-0.06	50th***	-0.05x+23.67	-0.07	-0.03
	75th**	-0.06x+34.73	-0.10	-0.03	75th*	-0.04x+34.58	-0.07	-0.02
	90th*	-0.12x+49.81	-0.19	-0.03	90th*	-0.08x+51.89	-0.15	-0.03
	95th	-0.07x+58.50	-0.16	0.12	95th	-0.06x+62.78	-0.13	0.00
L/W Ratio	5th	-0.01x+16.85	-0.04	0.01	5th	0.00x+5.17	-0.01	0.00
	10th	0.00x+18.58	-0.02	0.01	10th	0.00x+6.16	0.00	0.01
	25th	0.02x+21.91	0.00	0.03	25th	0.02x+16.51	0.00	0.04
	50th	0.02x+26.97	0.00	0.04	50th	0.02x+26.57	0.00	0.32
	75th	0.00x+34.79	-0.03	0.03	75th	0.03x+36.20	0.03	0.00
	90th	0.06x+43.60	0.00	0.10	90th	-0.03x+54.76	-0.09	0.07
	95th**	0.15x+49.39	0.03	0.22	95th	0.07x+73.91	-0.09	0.17

*$p \leq 0.05$, **$p \leq 0.01$, ***$p \leq 0.001$

Figure Legends

Figure 1. Map of the area off central California showing the locations where release experiments CO_2-4 and CO_2-5 were done.

Figure 2. A representation (not to scale) of the CO_2-4 experiment. Large, filled circles represent corrals, which were spaced ~ 4 m apart. The small, open circles represent cores. Two corrals were also sampled with single cores at their center.

Figure 3. A representation (not to scale) of the CO_2-5 experiment. Large, filled circles represent corrals; the diameter of the circle of corrals was ~15 m. The small, open circles represent cores. One corral was also sampled with a single core at its center.

Figure 4. Length plotted against diameter for all nematodes measured in collections from the CO_2-4 (upper figure) and CO_2-5 (lower figure) release experiments.

Figure 5. Nematode length:width ratio frequency distributions pooled across core layers and tail groups at various distance from a CO_2 source. Upper figure represents samples taken at 2 m, second figure at 4 m, third at 8 m, fourth at 21 m and bottom figure at 75 m from the CO_2 source.

Figure 6. Median individual length (µm ind^{-1}) (upper figure), diameter (µm ind^{-1}) (middle figure), and length/width ratio (lower figure) plotted against core layer for all nematodes measured in collections from the CO_2-4 (open circles) and CO_2-5 (open triangles) release experiments

Figure 7. Slope of quantile regressions as a function of tau (0.05-0.95) for nematode length, diameter, and L/W ratio vs. core layer for two release experiments. Shaded area represents the 95% confidence interval for each quantile to test the H_0: slope = 0 (i.e., no relationship between variable and sediment depth).

Figure 8. Median individual length (µm ind^{-1}) (upper figure), diameter (µm ind^{-1}) (middle figure), and length/width ratio (lower figure) plotted against distance from a source of CO_2 in two release experiments.

Figure 9. Slope of quantile regressions as a function of tau (0.05-0.95) for nematode length, diameter, and L/W ratio vs. distance from the CO_2 source for the two release experiments. Shaded area represents the 95% confidence interval for each quantile to test the H_0: slope = 0 (i.e., no relationship between variable and sediment depth).

Figure 10. Median individual length (µm ind^{-1}) (upper figure), diameter (µm ind^{-1}) (middle figure), and length/width ratio (lower figure) plotted against core layer for nematodes measured in collections at different distances from a source of CO_2 in two release experiments. Diamond symbols represent samples at 2 m, squares at 4 m, plus

signs at 8 m, triangles at 21 m, and circles at 75 m from the CO_2 source.

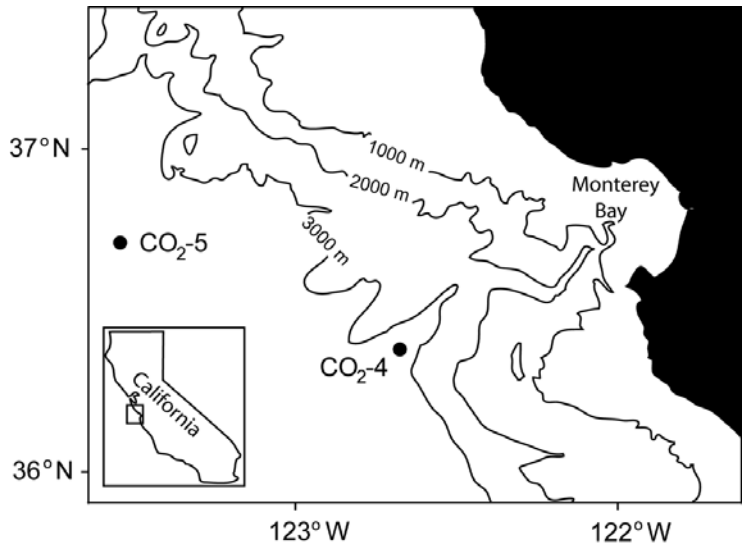
37°N
36°N
123° W
122° W
1000 m
2000 m
3000 m
Monterey
Bay
CO2-5
CO2-4
California

Figure 1

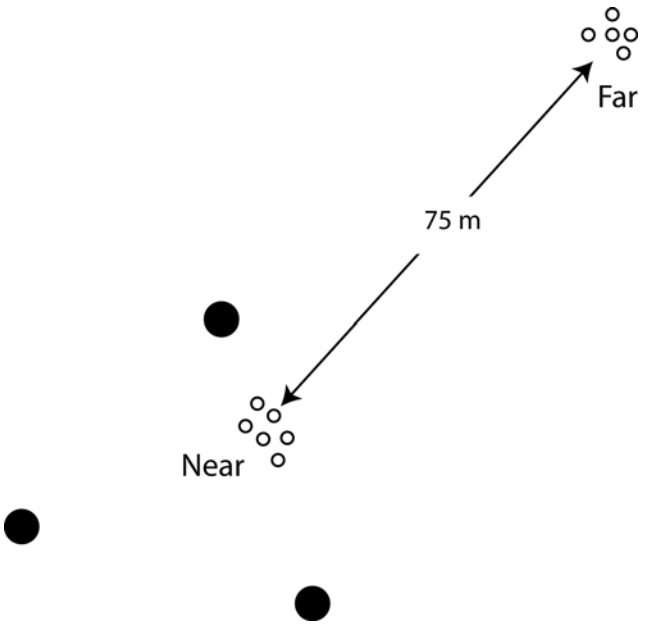

Figure 2

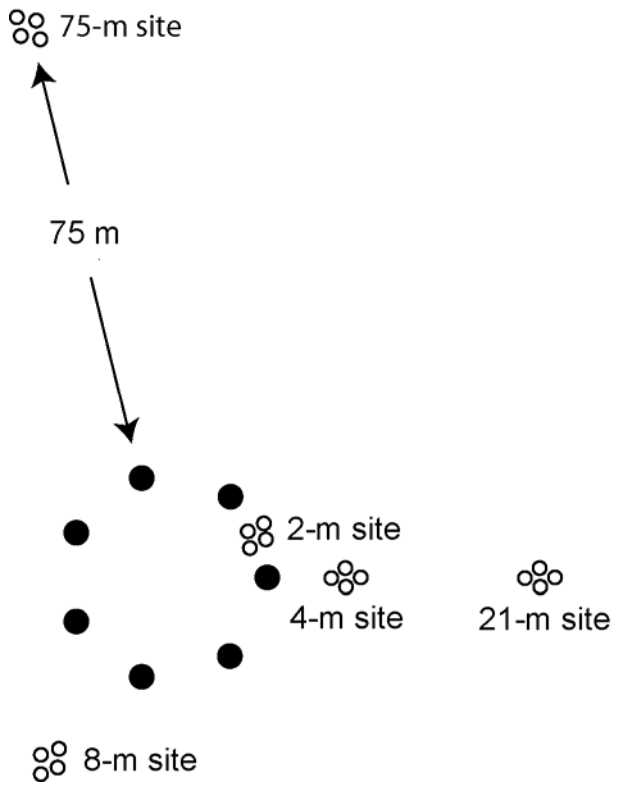

Figure 3

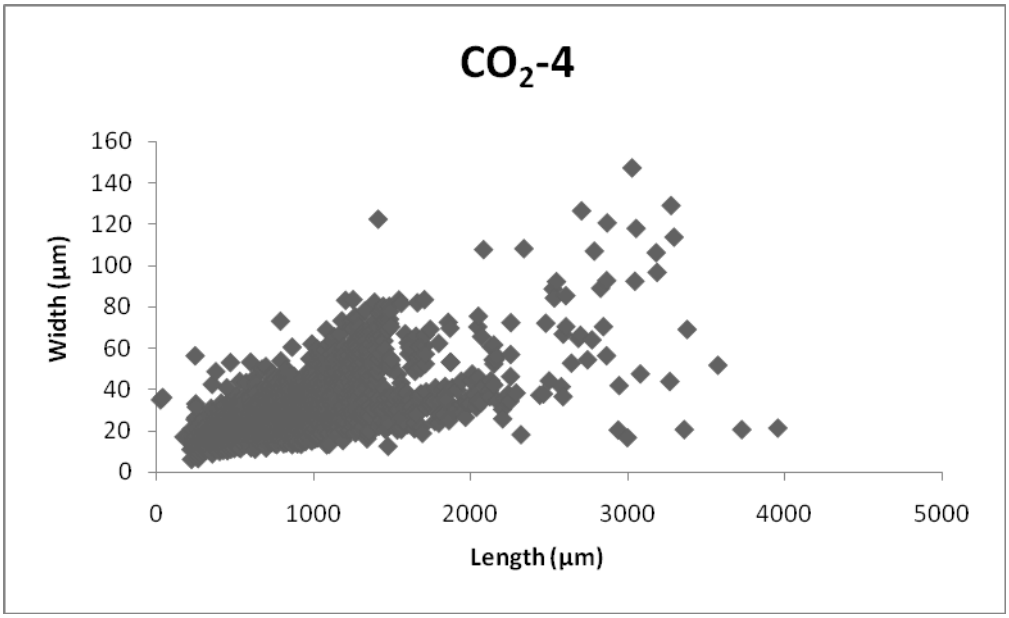
CO2-4
Width (µm)
Length (µm)
0
20
40
60
80
100
120
140
160
0
1000
2000
3000
4000
5000

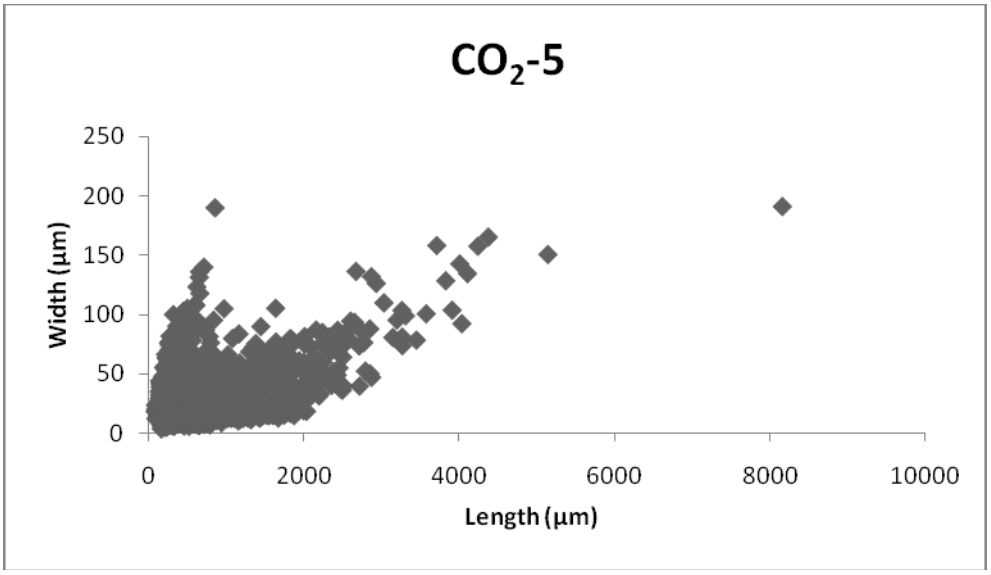
CO2-5
Width (µm)
Length (µm)
0
50
100
150
200
250
0
2000
4000
6000
8000
10000

Figure 4

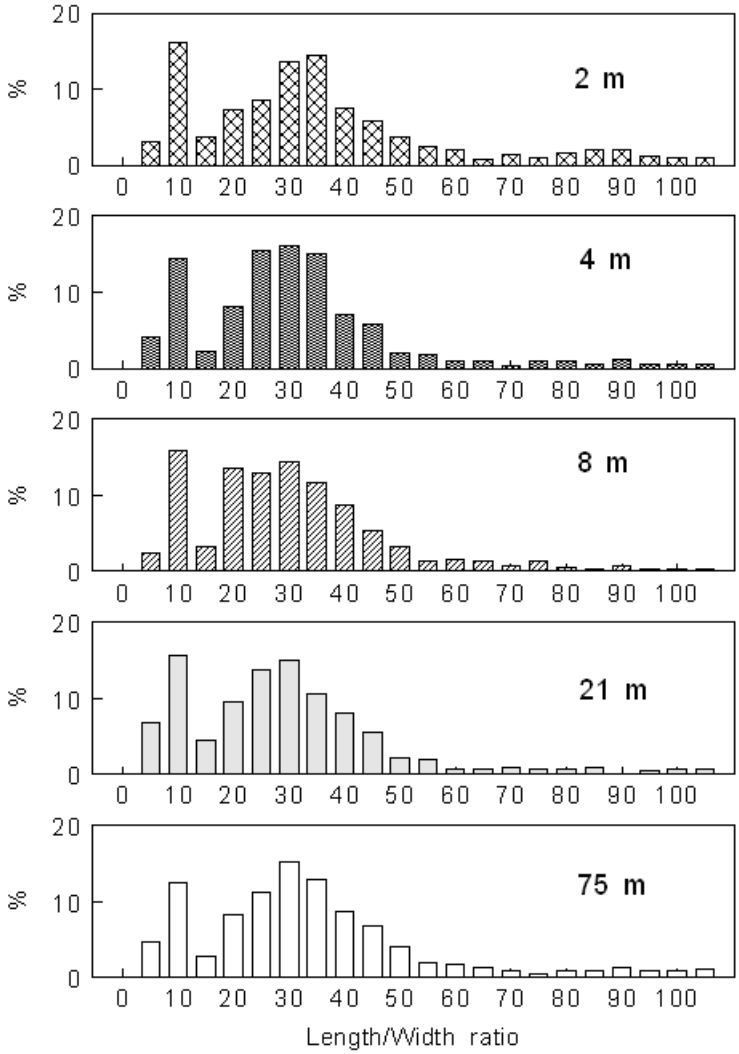
2 m
4 m
8 m
21 m
75 m
%
0
10
20
30
40
50
60
70
80
90
100
Length/Width ratio

Figure 5

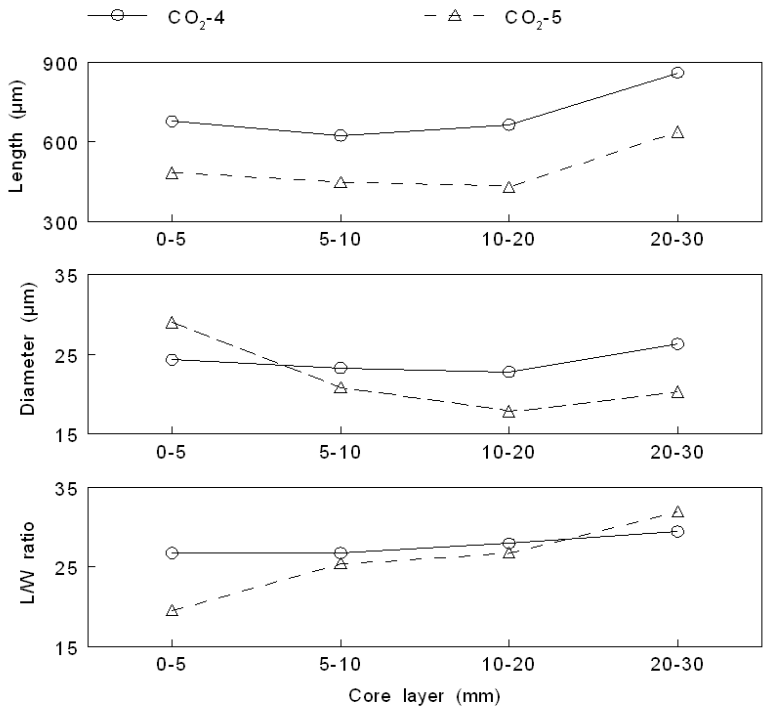
CO2-4
CO2-5
Length (μm)
900
600
300
0-5
5-10
10-20
20-30
Diameter (μm)
35
25
15
L/W ratio
Core layer (mm)

Figure 6

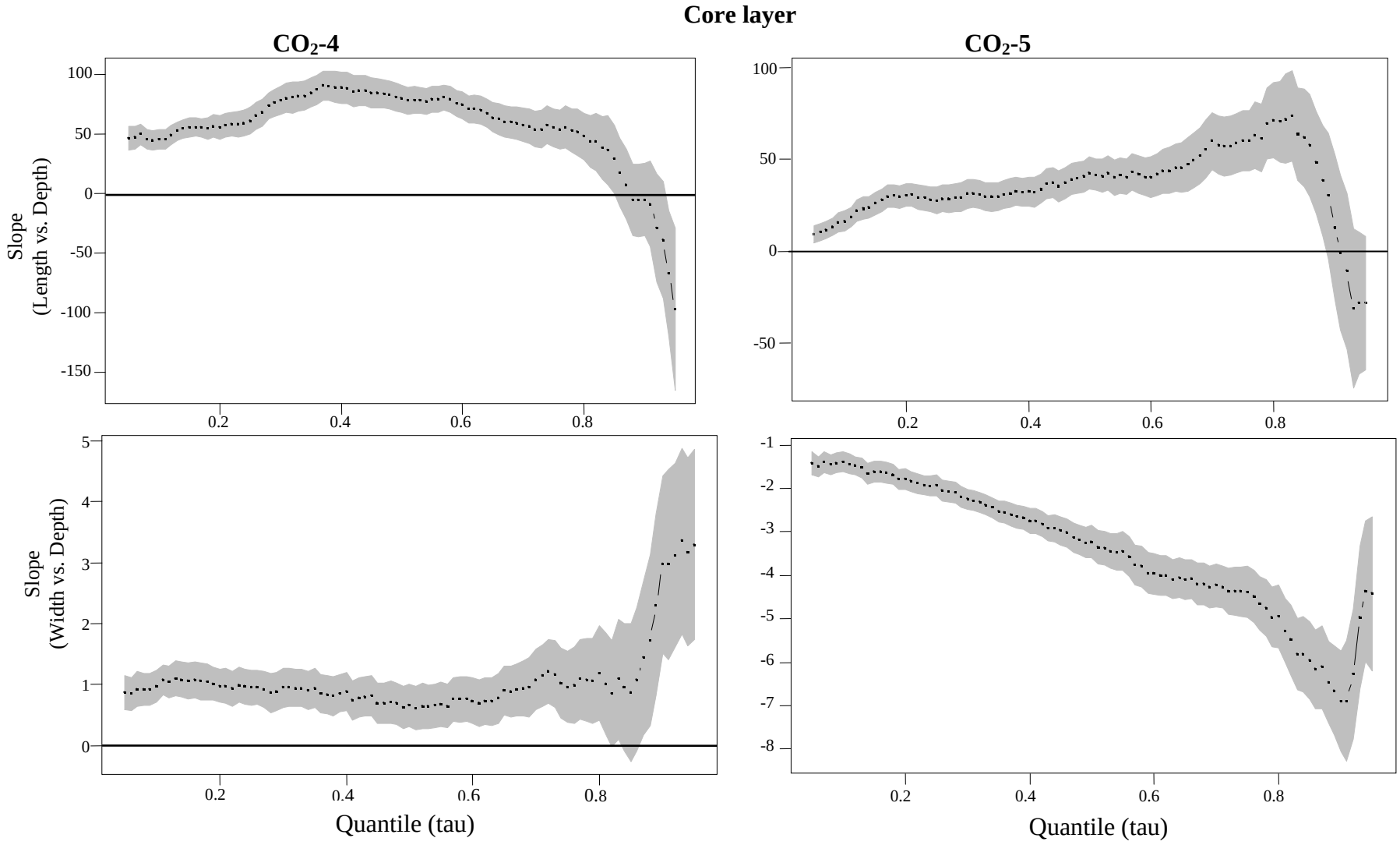
Core layer
CO2-4
CO2-5
Slope (Length vs. Depth)
Slope (Width vs. Depth)
Quantile (tau)
Quantile (tau)

Figure 7

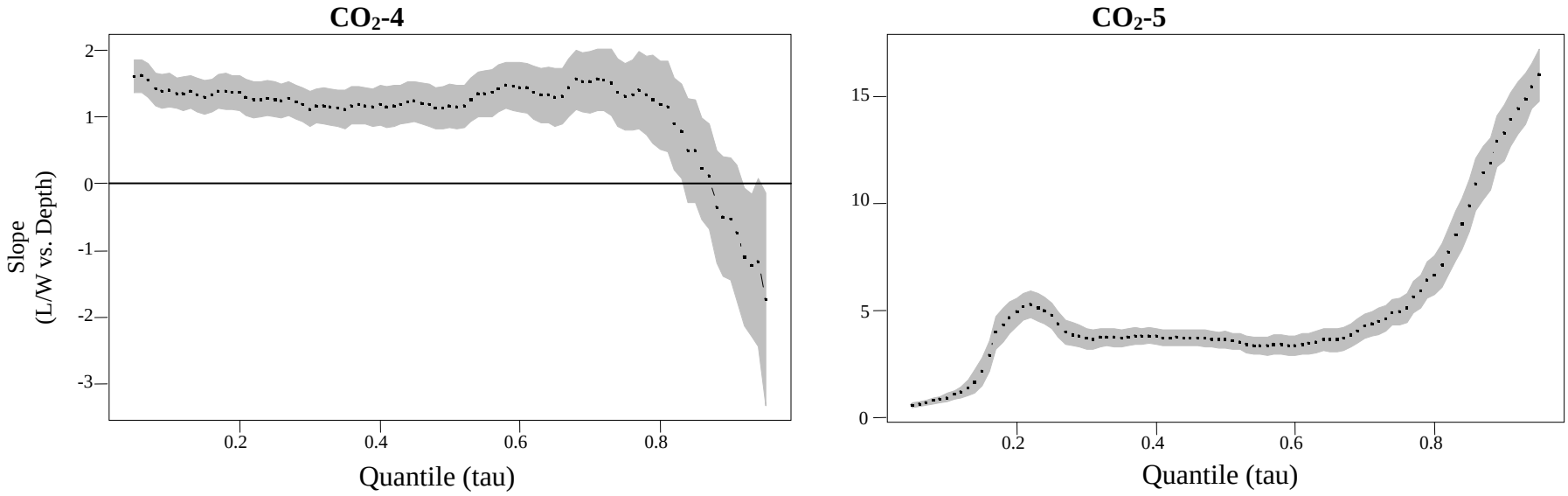

Figure 7, continued

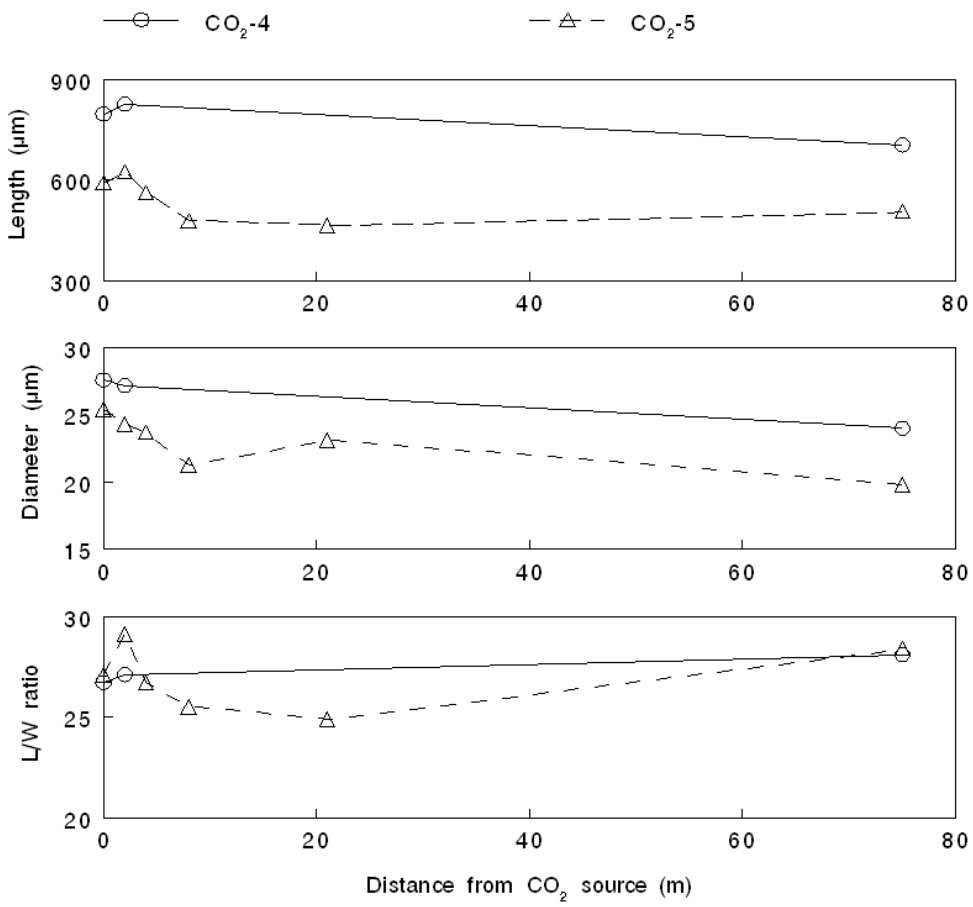
CO2-4
CO2-5
Length (µm)
900
600
300
0
20
40
60
80
Diameter (µm)
30
25
20
15
L/W ratio
Distance from CO2 source (m)

Figure 8

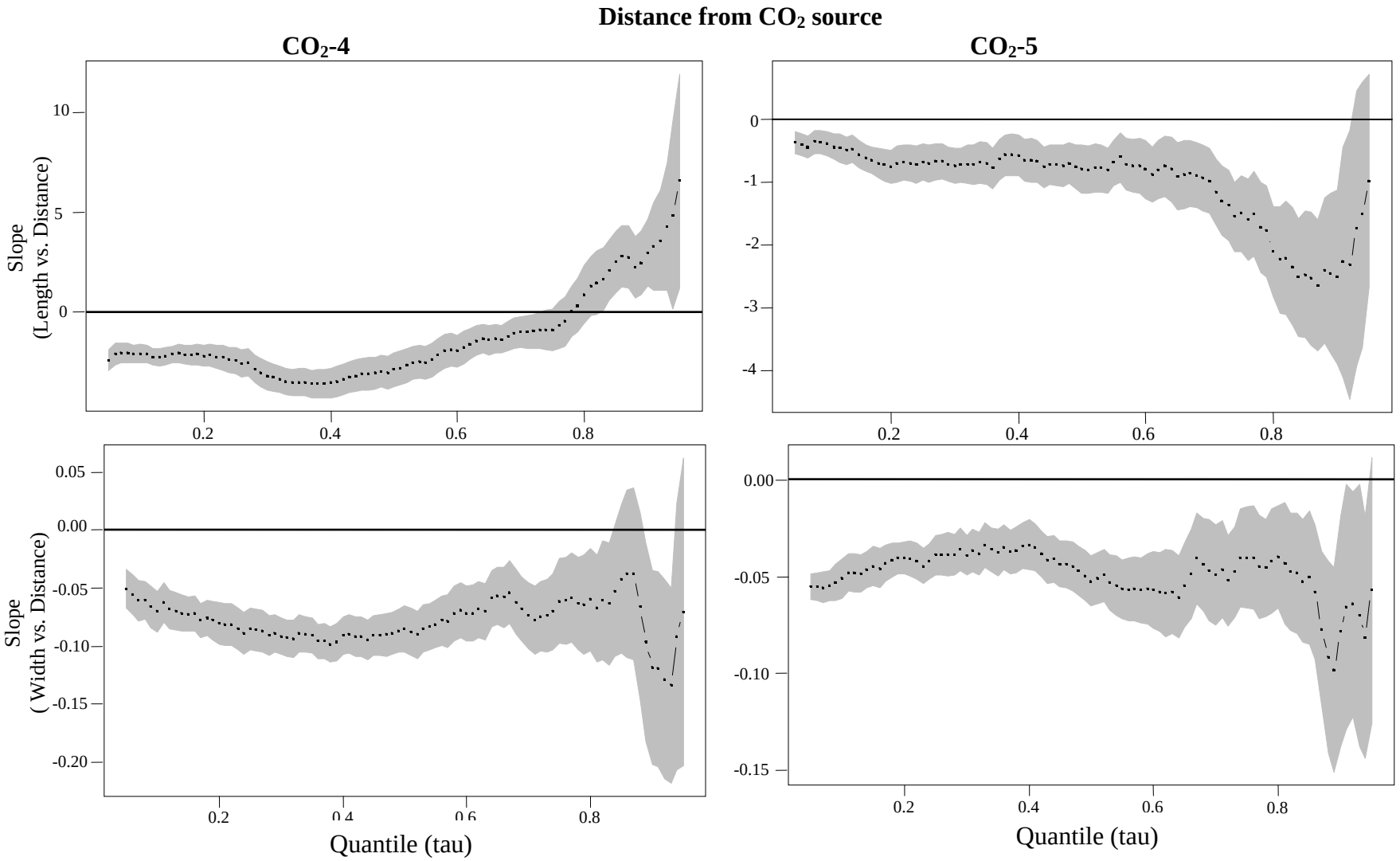
Distance from CO_2 source
CO_2-4
CO_2-5
Slope
(Length vs. Distance)
Slope
(Width vs. Distance)
Quantile (tau)
Quantile (tau)

Figure 9

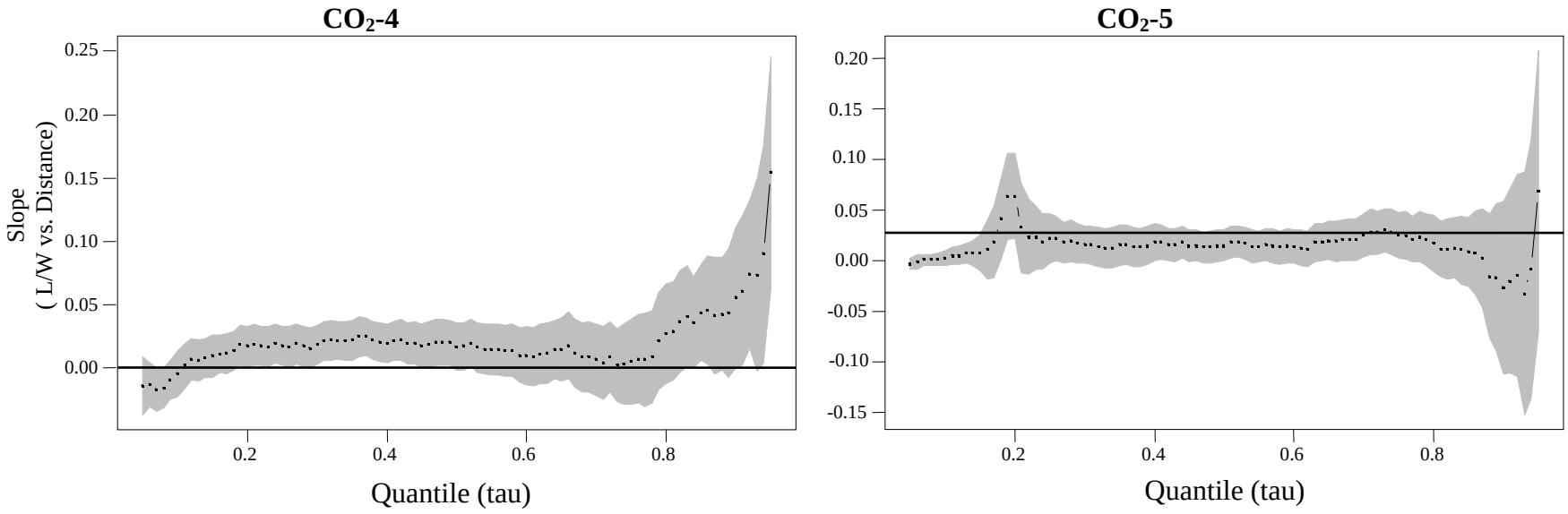

Figure 9, continued

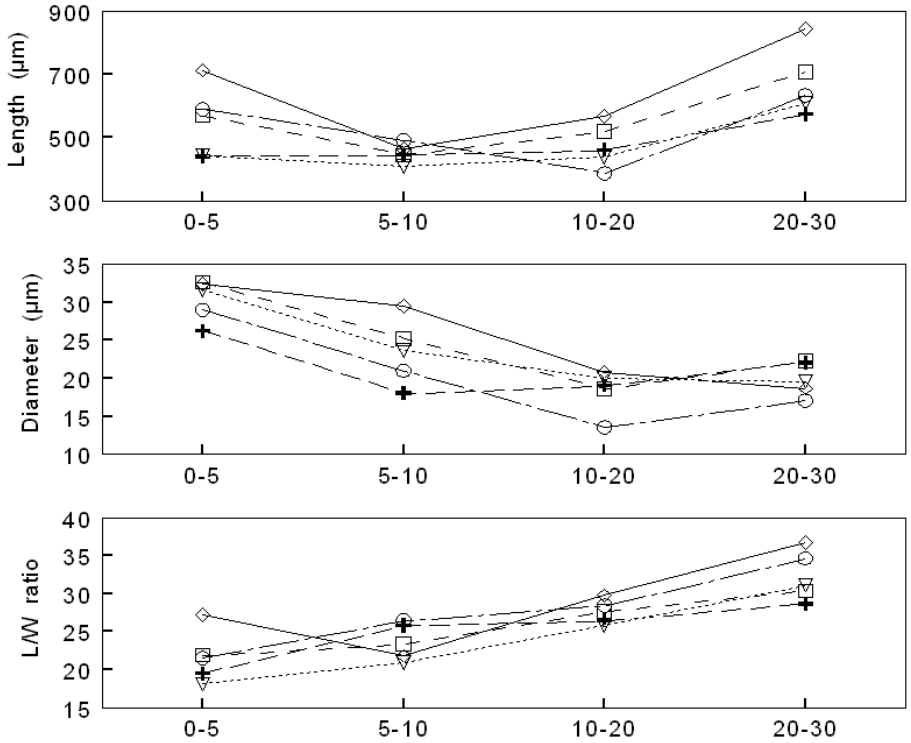
Length (µm)
900
700
500
300
0-5
5-10
10-20
20-30
Diameter (µm)
35
30
25
20
15
10
0-5
5-10
10-20
20-30
L/W ratio
40
35
30
25
20
15
0-5
5-10
10-20
20-30

Figure 10